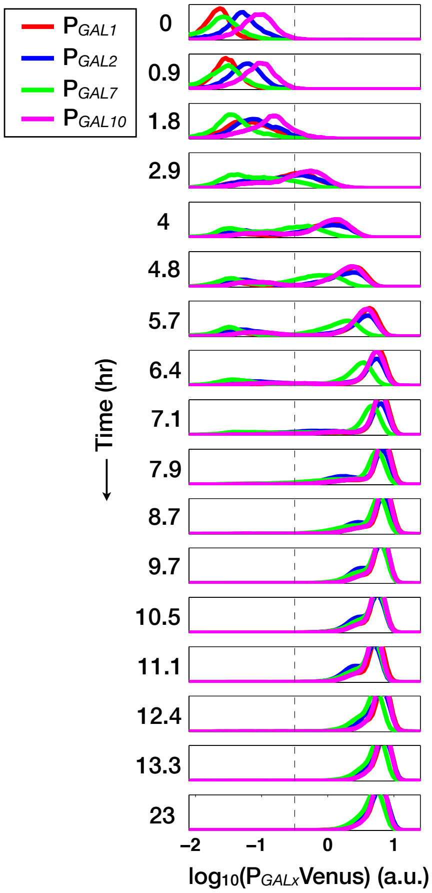

Supplementary Figure 1: Flow cytometry distributions of a fluorescent protein (Venus) fusion to the *GAL1*, *GAL2*, *GAL7* and *GAL10* promoters as a function of time in response to 0.1% glucose and 0.1% galactose. The dashed line denotes the threshold for computing the fraction of ON cells in Fig. 2.

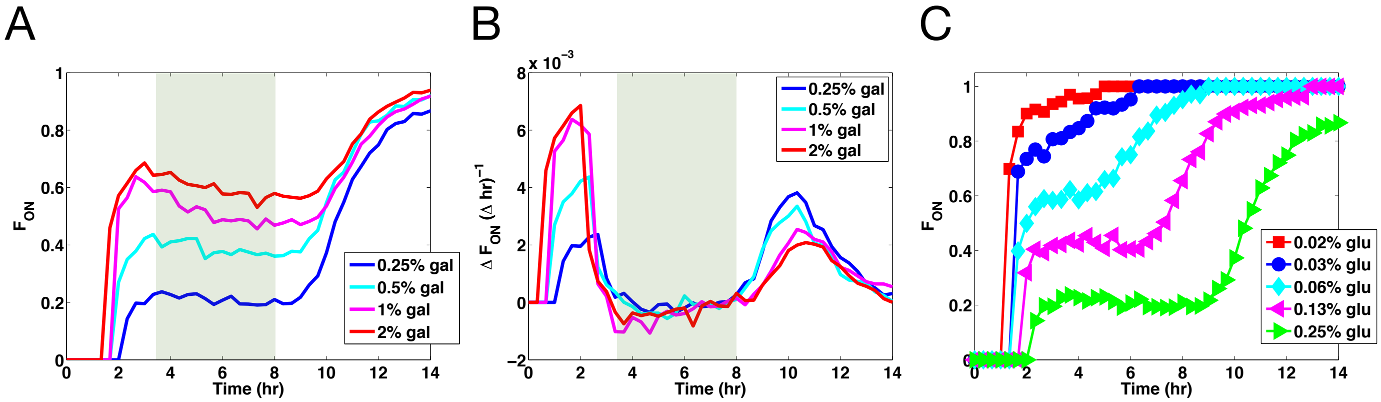

Supplementary Figure 2: Fraction of cells above a gene expression threshold ($\mathrm{F_{ON}}$, see Materials and Methods) as a function of time for a mixture of glucose and galactose. Cells were exposed to the two sugars simultaneously at time zero. **(A)** $\mathrm{F_{ON}}$ as a function of time in response to 0.25% glucose and a range of galactose concentrations. Highlighted box in **A** and **B** indicates bimodal region. **(B)** Rate of change of $\mathrm{F_{ON}}$ as a function of time for data shown in **A**. **(C)** $\mathrm{F_{ON}}$ as a function of time in response to 0.25% galactose and a range of glucose concentrations.

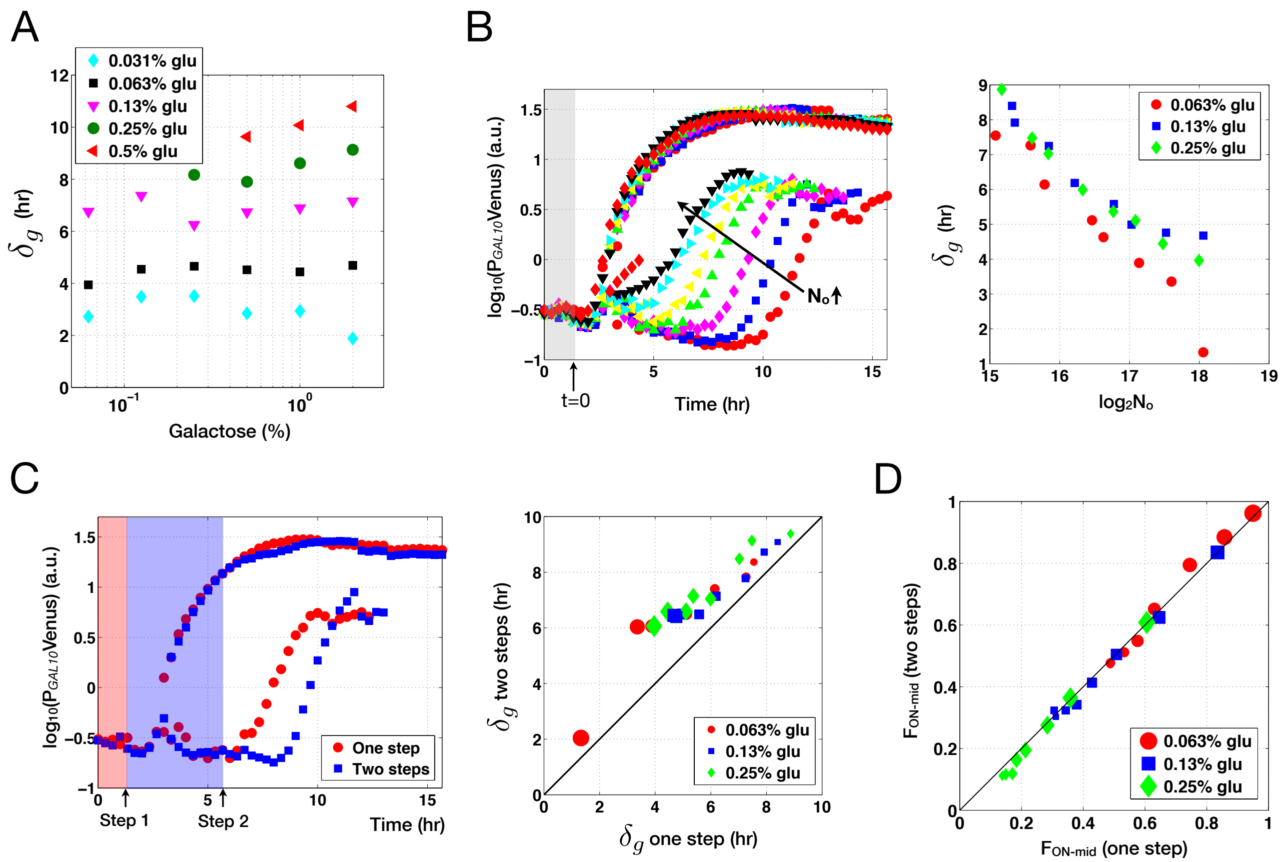

Supplementary Figure 3: Experimentally measured dynamic features of the GAL system as a function of glucose and galactose. **(A)** Duration of bimodality (δ_g) as a function of galactose for different glucose concentrations. **(B)** Means of the ON and OFF subpopulations over time quantified using a Gaussian mixture model (GMM) for 0.063% glucose and 0.25% galactose for a range of initial cell densities (N_o, values shown in right panel). Each marker represents a culture that was initialized at a different N_o (arrow highlights that increasing N_o decreases the duration of bimodality – δ_g). The right panel quantifies the relationship between the values of N_o and δ_g. **(C)** Two steps of glucose produces a larger δ_g. Means of the OFF and ON subpopulations as a function of time for cultures that either received a single step of 0.063% glucose (red circles) or two steps of 0.063% glucose (one at time zero and the second after 5 hours, blue squares). Both cultures received 0.25% galactose at time zero. Right panel: quantification of δ_g across a range of N_o for three glucose concentrations in conditions with a single or two steps of glucose. All conditions received 0.25% galactose from time zero. Data point size is proportional to N_o. **(D)** Comparison of the fraction of ON cells at the midpoint of the transient bimodal region ($F_{\text{ON-mid}}$, see Materials and Methods) across a range of N_o for three glucose concentrations for conditions that received one or two steps of glucose. All conditions received 0.25% galactose from time zero. Data point size is proportional to N_o.

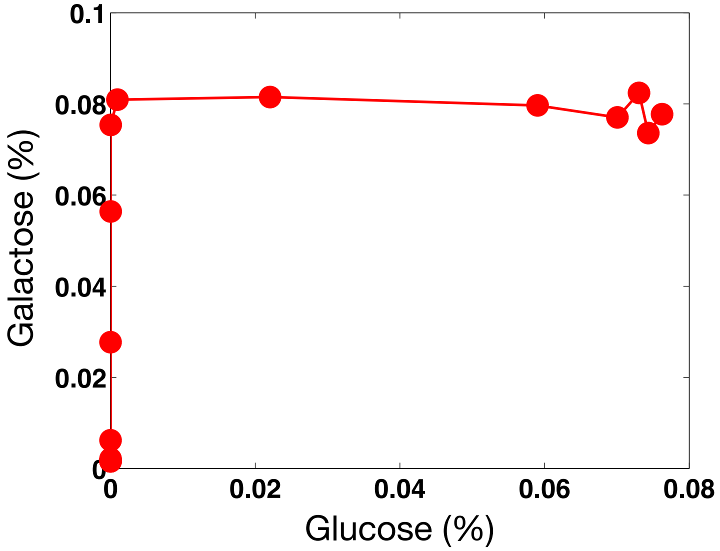

Supplementary Figure 4: Time series measurements of glucose and galactose concentrations of a wild type strain expressing p*GAL10*-Venus.

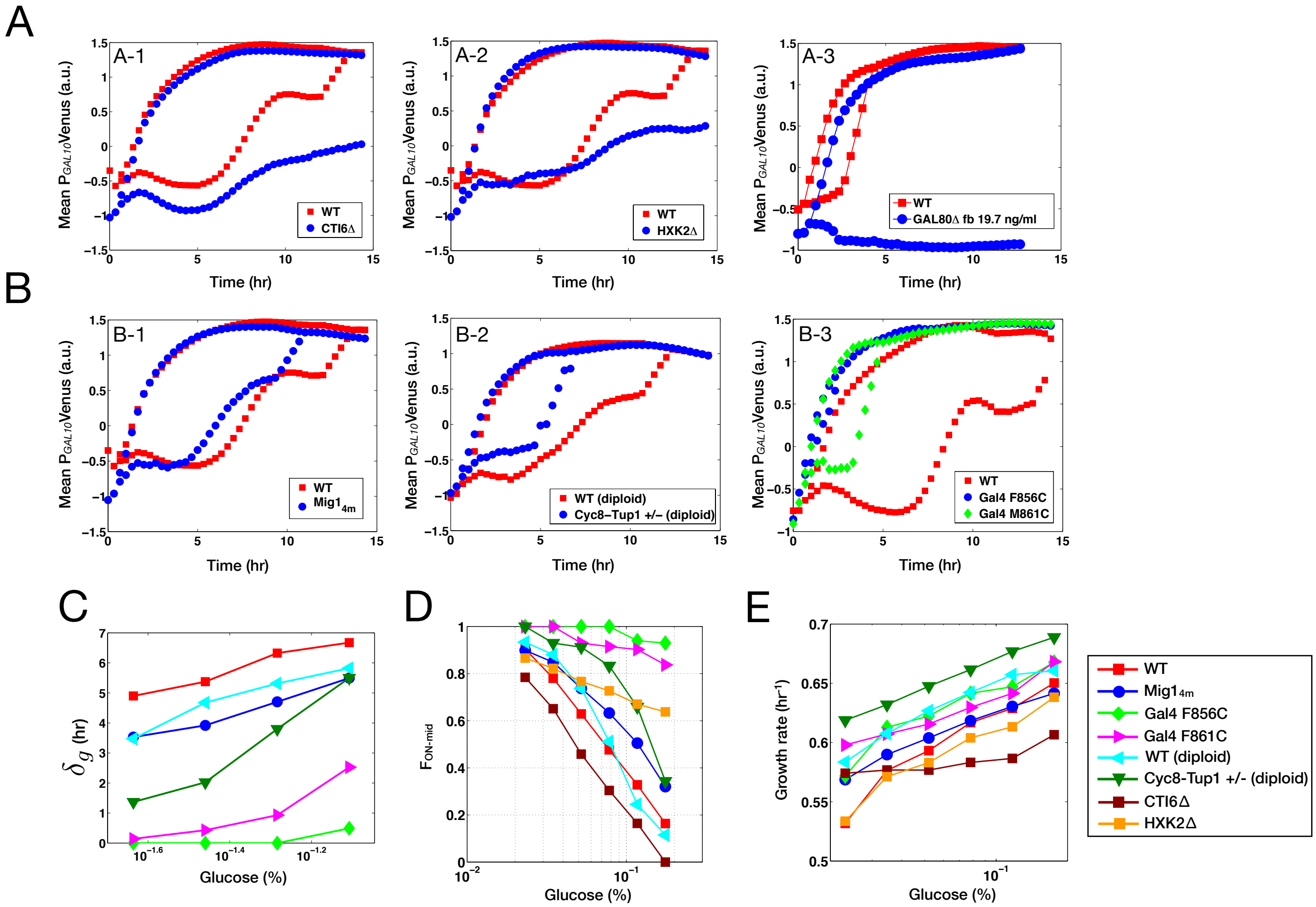

Supplementary Figure 5: Modulation of the duration of bimodality (δ_g) and fraction of ON cells at the midpoint of the transient bimodal region ($F_{\text{ON-mid}}$, see Materials and Methods) in a panel of mutants. **(A)** Means of the ON and OFF subpopulations for a set of mutants that exhibited a larger δ_g compared to wild type. These mutants include gene deletions of *CTI6* (A-1) and *HXK2* (A-2) in response to a step input of 0.05% glucose and 0.13% galactose. Disruption of the feedback loop of *GAL80* by a deletion of this gene and expression of *GAL80* from an inducible aTc-responsive promoter (19.7 ng/ml aTc, GAL80Δ fb) prevents the OFF subpopulation from activating for the duration of the experiment in the presence of 0.06% glucose and 0.5% galactose (A-3). **(B)** Means of the ON and transiently OFF subpopulations for a set of mutants that exhibited a smaller δ_g compared to WT. These mutants include a quadruple point mutant of Mig1p (Mig1$_{4m}$) that reduces the affinity of Mig1p to the general repression complex Cyc8-Tup1 (B-1) in response to 0.05% glucose and 0.13% galactose, hemizygous mutant of *CYC8-TUP1* in a diploid strain compared to a wild type diploid (B-2) for a step input of 0.05% glucose and 0.13% galactose and single point mutants of Gal4p (F856C and M861C) with reduced affinity to Gal80p (B-3) for a step input of 0.08% glucose and 0.13% galactose. **(C)** Quantification of δ_g in response to a step of 0.13% galactose and a range of glucose levels. δ_g could not be quantified for mutants in **A** that exhibited an OFF subpopulation that never switched to the ON state over the course of the experiment. **(D)** $F_{\text{ON-mid}}$ for the same mutants and doses of glucose and galactose as panel **C**. **(E)** Growth rates of the mutant strains. Growth rates were computed by linear regression on the number of cells collected at each time point averaged over a period of 12 hours.

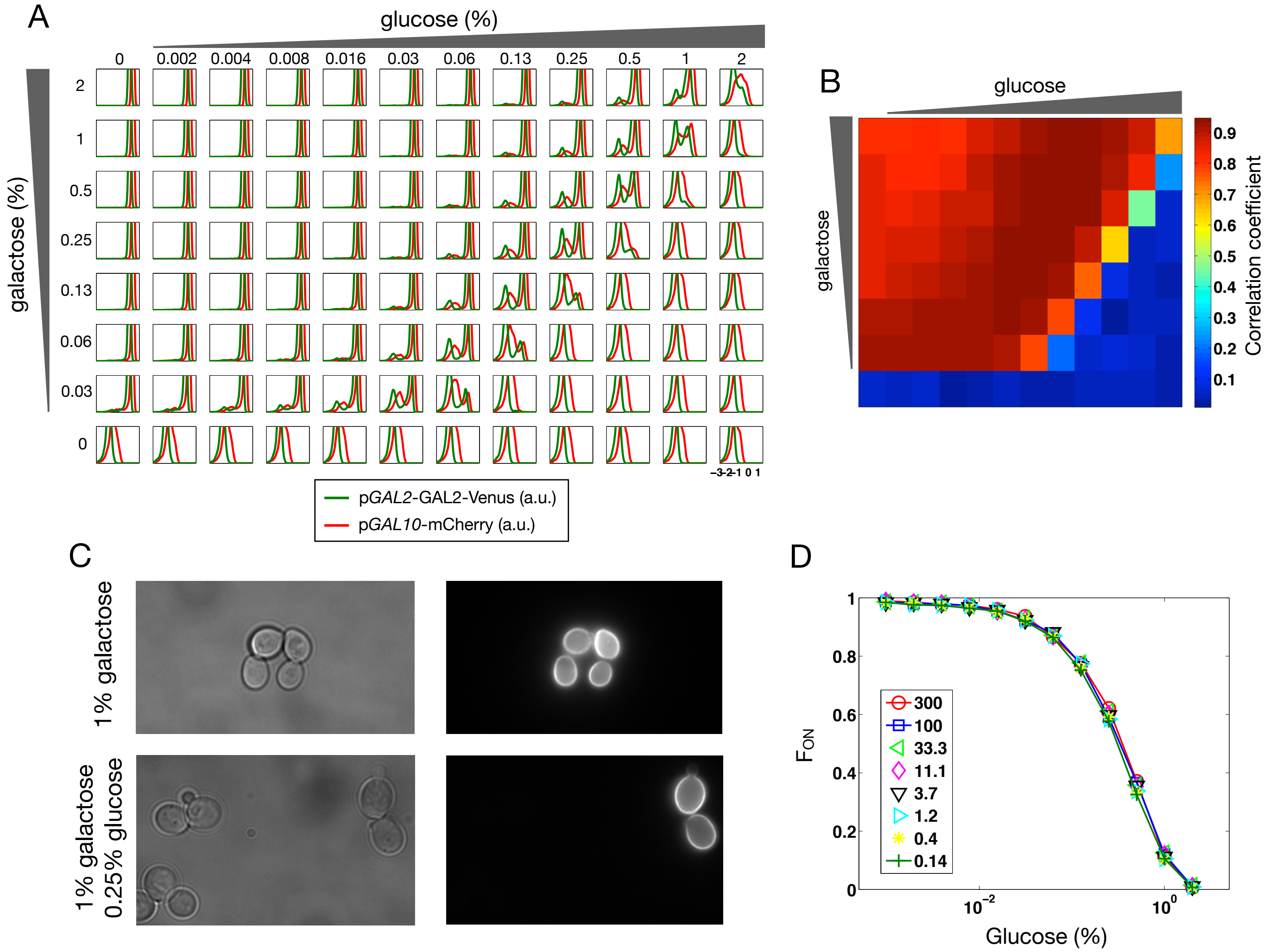

Supplementary Figure 6: The protein levels of the *GAL2* permease strongly correlate with a *GAL10* promoter fusion in response to a mixture of glucose and galactose. **(A)** Flow cytometry distributions of a single strain expressing both a fluorescent protein fusion of Venus to Gal2p (p*GAL2*-GAL2-Venus) and a promoter fusion of mCherry to the *GAL10* promoter (p*GAL10*-mCherry) following a 5 hour induction with different combinations of glucose and galactose. **(B)** Heat-map of correlation coefficients of p*GAL2*-GAL2-Venus and p*GAL10*-mCherry for the distributions shown in **A**. **(C)** Microscopy images of wild-type cells expressing p*GAL2*-GAL2-Venus exposed to either 1% galactose (top) or 1% galactose + 0.25% glucose (bottom) for 4 hours. **(D)** Relationship between the Gal2p expression level and the fraction of ON cells (F_{ON}) in a strain deleted for the endogenous *GAL2* gene and expressing Gal2p from an aTc inducible TET promoter and p*GAL10*-Venus reporter (GAL2Δ fb). Cells were exposed to 0.5% galactose and a range of glucose concentrations and aTc levels (ng/μl) for 6 hours.

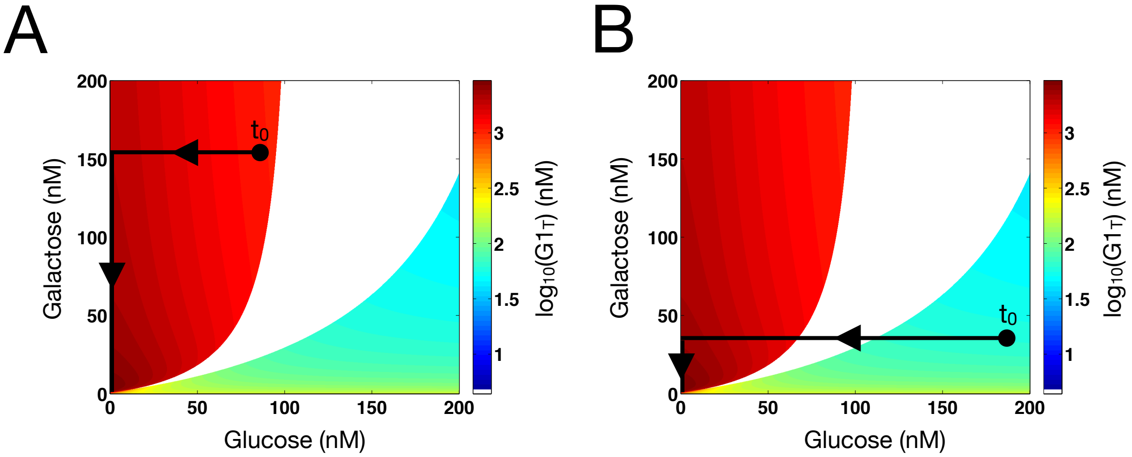

Supplementary Figure 7: Initialization of the GAL model with glucose inhibition in different concentration regimes of glucose and galactose generates distinct dynamic responses. Time zero is denoted by t_0. The solid line illustrates the sequential consumption of glucose and galactose as a function of time. The colored regions denote monostability and the white region represents bistability. In the colored regions, red indicates monostable ON corresponding to high total G1 levels ($G1_T$) and blue represents monostable OFF corresponding to low $G1_T$. **(A)** Representative dynamic trajectory in response to galactose and a sufficiently low initial glucose concentration. **(B)** Representative dynamic trajectory in response to an initial glucose concentration that is significantly higher than the initial galactose level.

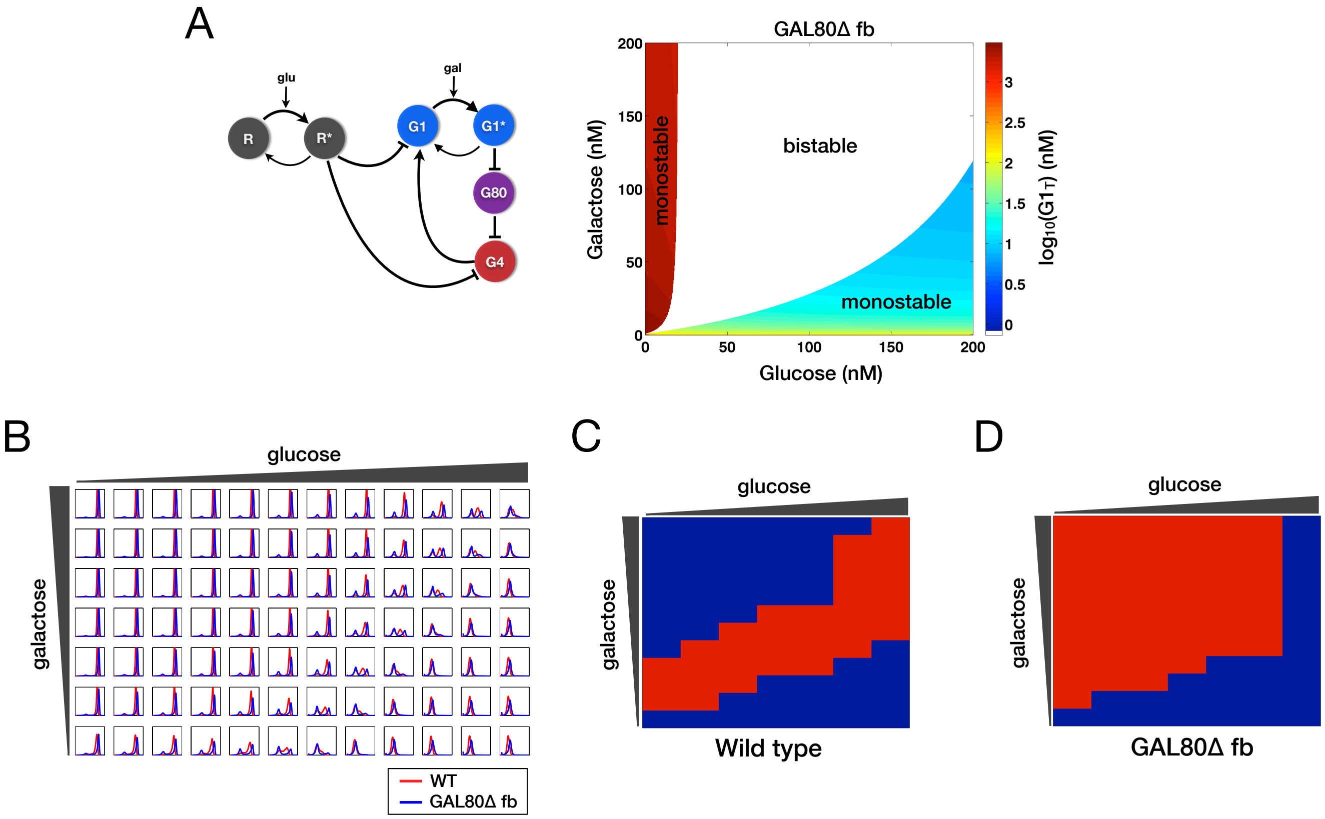

Supplementary Figure 8: Removal of the *GAL80* feedback loop expands the region of bistability across different concentrations of glucose and galactose in the computational model. This feature is corroborated by experimental measurements of a strain in which the *GAL80* gene is deleted and this gene is expressed from an inducible aTc-responsive promoter in response to 0 ng/ml aTc (GAL80Δ fb). This level of constitutive Gal80p expression corresponds to approximately 40% of fully induced wild type levels [2]. **(A)** Circuit diagram of the GAL80Δ fb model (left, see supplementary text). Bifurcation diagram of the regions of monostability (colored) and bistability (white) for different values of glucose and galactose (right). The model predicts that removing the *GAL80* feedback loop expands the range of glucose and galactose concentrations that produce bistability. **(B)** Single-cell fluorescence distributions of p*GAL10*-Venus in the wild type and GAL80Δ fb. **(C)** Gaussian mixture model (GMM) classification (see Materials and Methods) of experimentally measured p*GAL10*-Venus gene expression distributions shown in **B** for the wild type. Red and blue represent a bimodal and monomodal distribution, respectively. **(B)** GMM classification of experimentally measured fluorescence distributions in **B** for GAL80Δ fb.

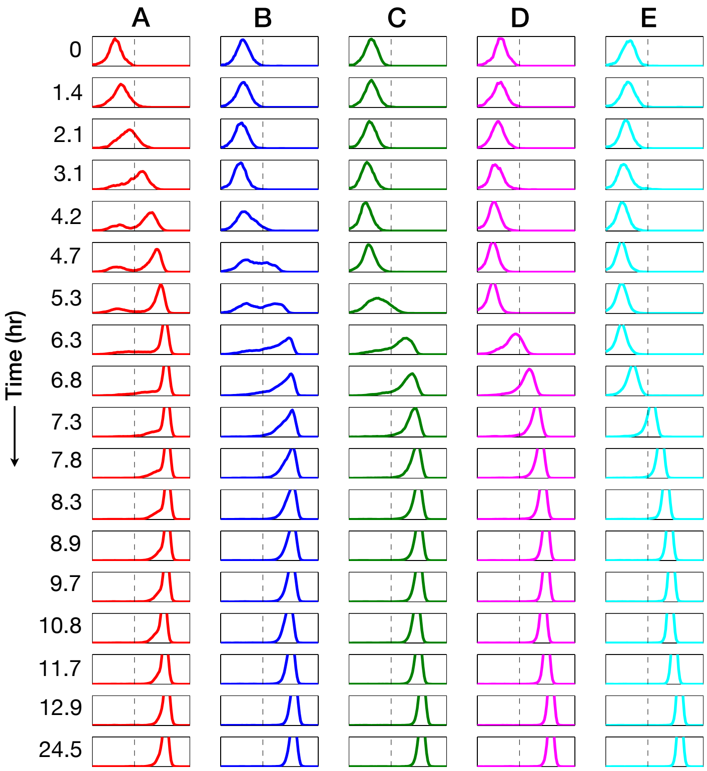

Supplementary Figure 9: Single-cell fluorescence distributions of p*GAL10*-Venus in the wild type for conditions A-E in the delayed galactose experiment (Fig. 3,4). The dotted lines denote the threshold used to compute the fraction of ON cells in Fig. 3.

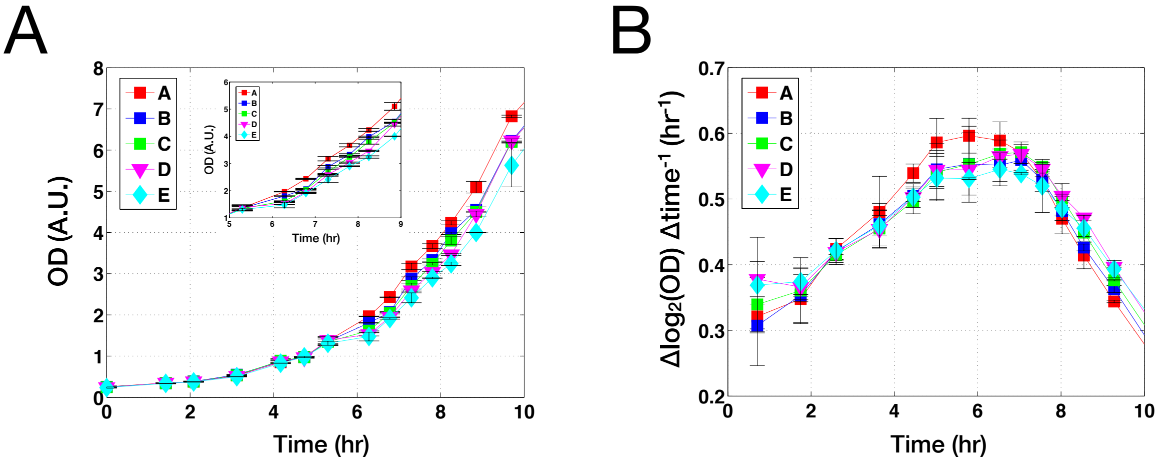

Supplementary Figure 10: Optical density (OD) and growth rates over time for the delayed galactose experiment (Fig. 3,4). **(A)** Optical density over time. Inset shows an enlarged region of the lag phase in growth. **(B)** Rate of change of the log of the OD as a function of time.

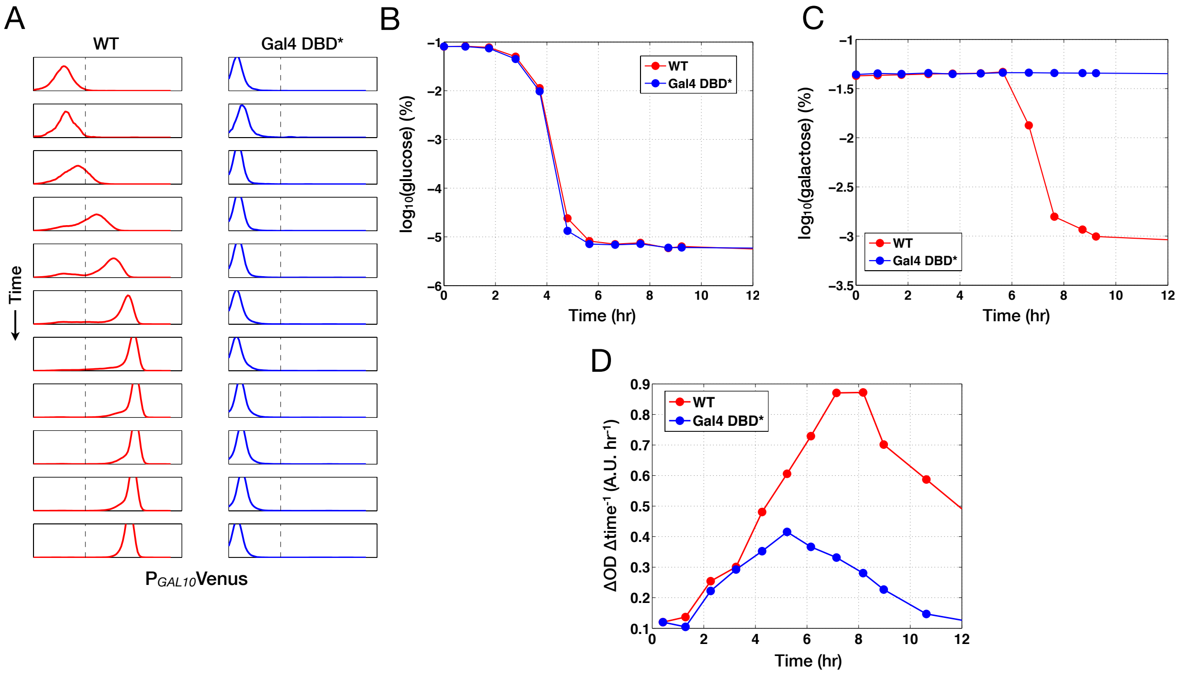

Supplementary Figure 11: Galactose does not benefit cells until glucose is consumed for a mutant strain in which the *GAL4* gene is deleted and a point mutant of *GAL4* (C14Y) is expressed that is unable to activate GAL gene expression (Gal4 DBD*). Cells were exposed to 0.1% glucose and 0.1% galactose at time zero. **(A)** Single-cell fluorescence distributions of a p*GAL10*-Venus in the wild type and Gal4 DBD*. **(B)** Glucose concentrations as a function of time. Lines represent fitted Hill functions. **(C)** Galactose concentrations as a function of time. **(D)** Growth rates as a function of time.

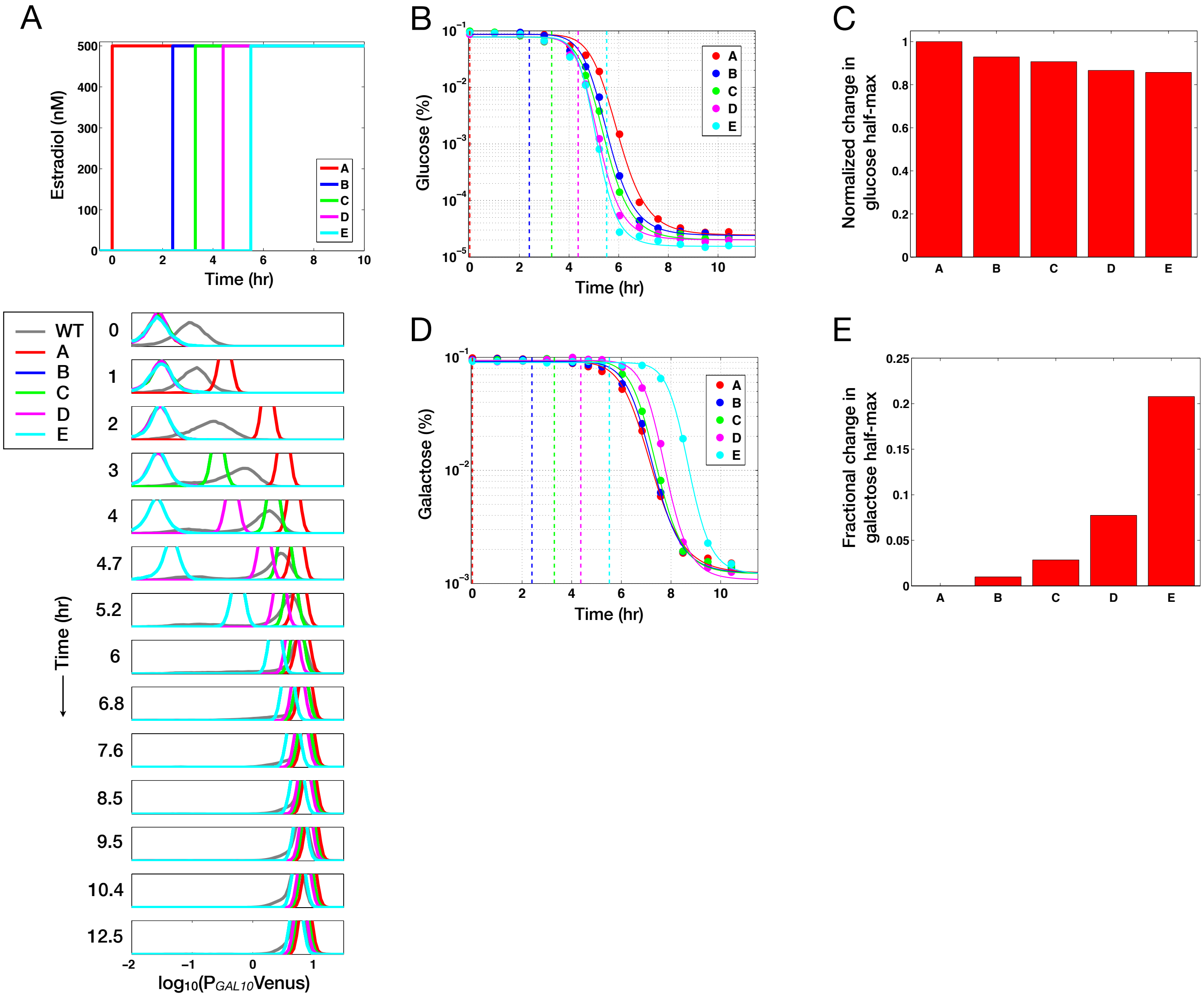

Supplementary Figure 12: Early activation of the GAL genes using an estradiol inducible Gal4 chimera prior to glucose depletion reduces the rate of glucose consumption and accelerates galactose consumption. **(A)** Experimental design. Each condition (A-E) received a step input of 0.1% glucose and 0.1% galactose at time zero and 500 nM estradiol to activate the Gal4 chimera at the indicated times (top). Single-cell fluorescence distributions of p*GAL10*-Venus as a function of time (bottom). **(B)** Glucose concentrations as a function of time. Lines represent fitted Hill functions. Dashed lines indicate the time when estradiol was added to each culture. **(C)** Normalized change in the half-max of the glucose consumption curves for the different conditions relative to condition A. **(D)** Galactose concentrations as a function of time. **(E)** Fractional change in the half-max of the galactose concentration curves relative to condition A.

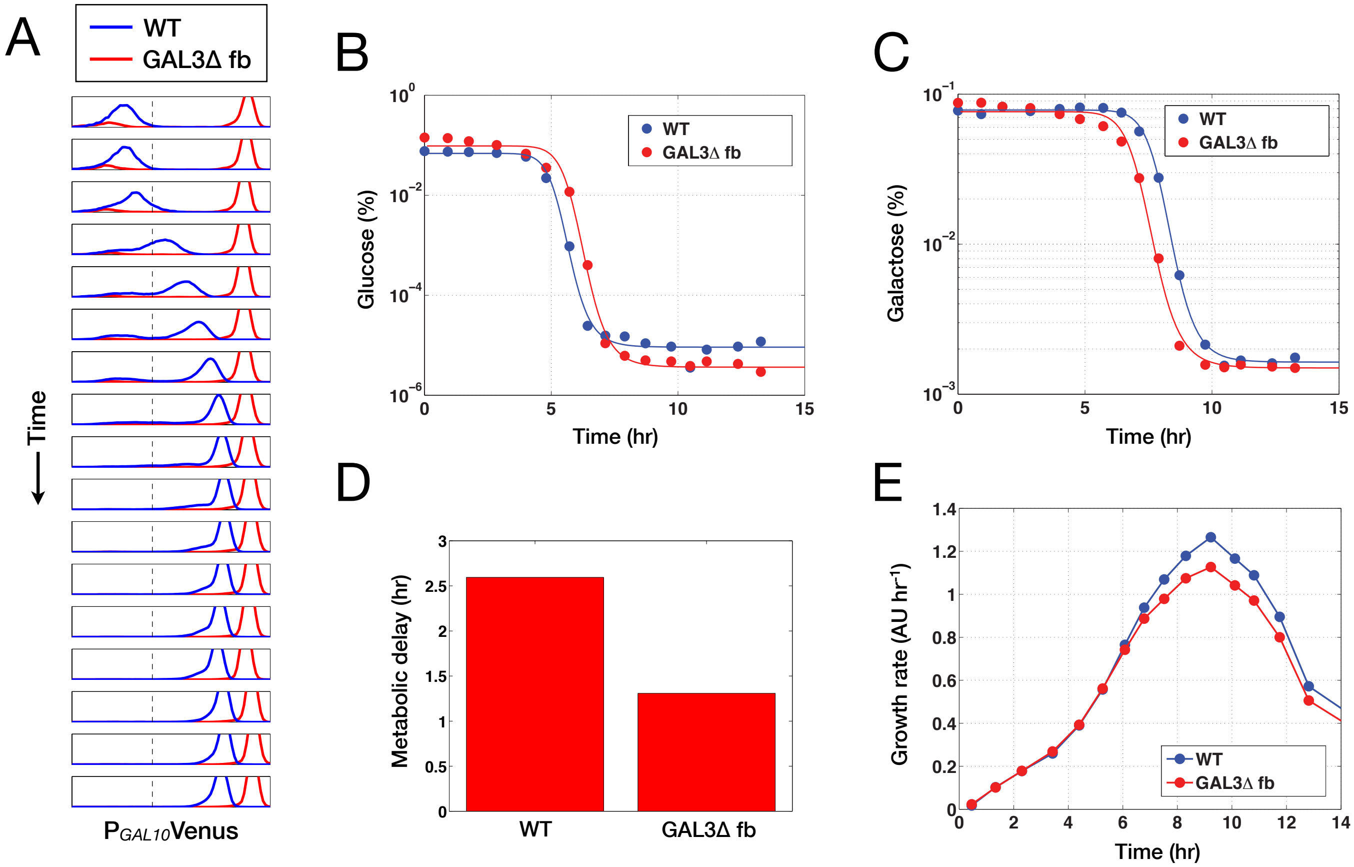

Supplementary Figure 13: Modification of sugar metabolism and growth by constitutive GAL gene expression. The GAL pathway was induced approximately 12 hours in advance of the wild type using a strain in which *GAL3* is deleted and this gene is expressed from an inducible aTc-responsive promoter (450 ng/ml aTc, GAL3Δ fb). At time zero, the GAL3Δ fb and wild type strains received 0.1% glucose and 0.1% galactose. **(A)** Single-cell fluorescence of p*GAL10*-Venus in wild type and GAL3Δ fb. **(B)** Glucose concentrations as a function of time. Lines represent fitted Hill functions. **(C)** Galactose concentrations as a function of time. **(D)** Metabolic delay for wild type and GAL3Δ fb computed by subtracting the half-max of the glucose and galactose curves. **(E)** Growth rates as a function of time.

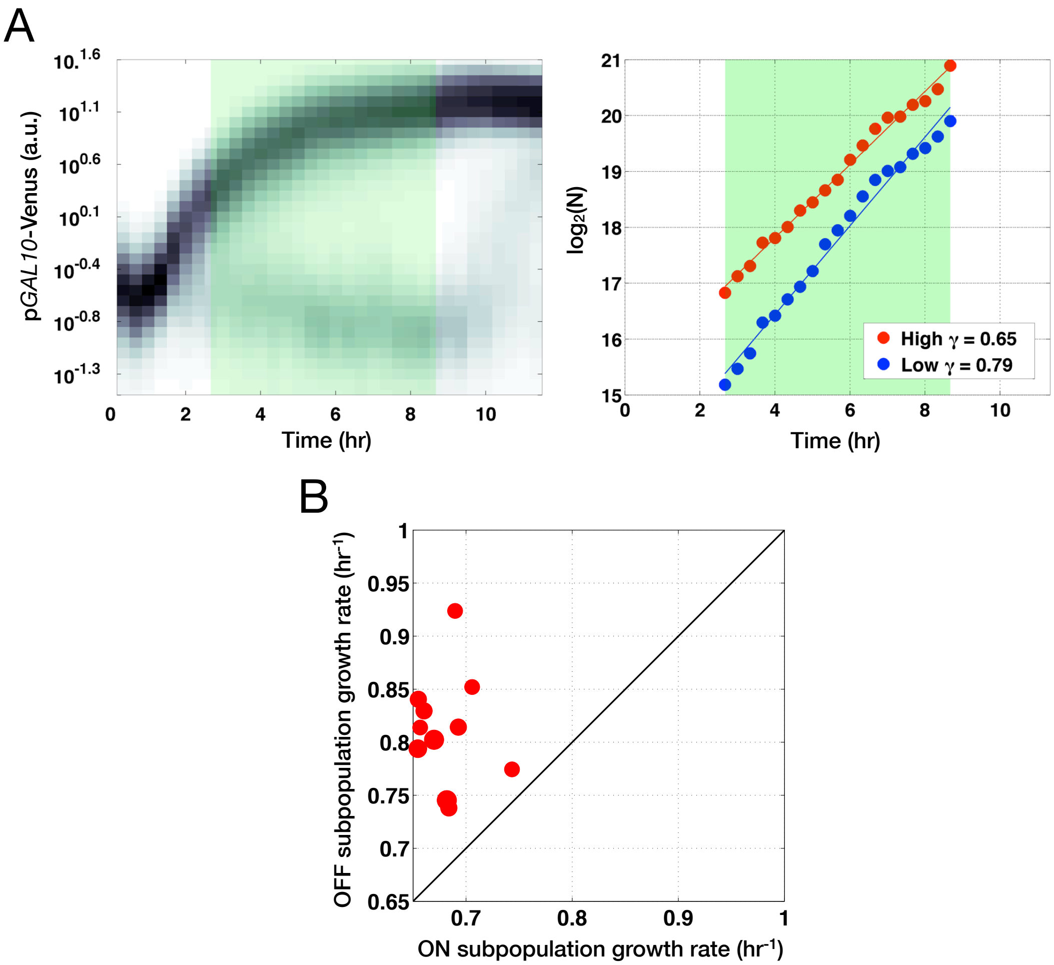

Supplementary Figure 14: The GAL OFF subpopulation grows faster than the GAL ON subpopulation. **(A)** Representative dynamic flow cytometry measurements of p*GAL10*-Venus in response to 0.5% glucose and 1% galactose from the experiment in Fig. 1. Heatmap of fluorescence distributions as a function of time (left). Quantification of the number of cells in the OFF and ON subpopulations (right, see Materials and Methods). $\text{Log}_2(\text{N})$ as a function of time. N represents the number of cells in the GAL ON or OFF subpopulations. **(B)** Growth rate of GAL OFF subpopulation versus the GAL ON subpopulation for different initial concentrations of glucose and galactose. The diameter of each data point is proportional to the initial concentration of glucose.